Cyclic Block Copolymers for Controlling Feature Sizes in Block Copolymer Lithography

Justin E. Poelma,[†,‡] Kosuke Ono,[†,§] Daigo Miyajima,[†,⊥] Takuzo Aida,[⊥] Kotaro Satoh,[†,∥] and Craig J. Hawker[†,‡,#,*]

[†]Materials Research Laboratory, University of California, Santa Barbara, California 93106, United States, [‡]Materials Department, University of California, Santa Barbara, California 93106, United States, [§]Department of Chemistry, Tokyo Institute of Technology, 2-12-1, O-okayama, Meguro-ku, Tokyo 152-8551 Japan, [⊥]Department of Chemistry and Biotechnology, The University of Tokyo, Tokyo, Japan, [∥]Department of Applied Chemistry, Nagoya University, Furo-cho, Chikusa-ku, Nagoya 464-8603, Japan, and [#]Department of Chemistry and Biochemistry, University of California, Santa Barbara 93106, United States

ABSTRACT Block copolymer lithography holds promise as a next-generation technique to achieve the sub-20 nm feature sizes demanded by semiconductor roadmaps. While molecular weight and block immiscibility have traditionally been used to control feature size, this study demonstrates that macromolecular architecture is also a powerful tool for tuning domain spacing. To demonstrate this concept, a new synthetic strategy for cyclic block polymers based on highly efficient "click" coupling of difunctional linear chains is developed, and the thin film self-assembly of cyclic polystyrene-*block*-polyethylene oxide (cPS-*b*-PEO) is compared with the corresponding linear analogues. The reduced hydrodynamic radii of the cyclic systems result in ~30% decrease in domain spacing over the corresponding linear polymers.

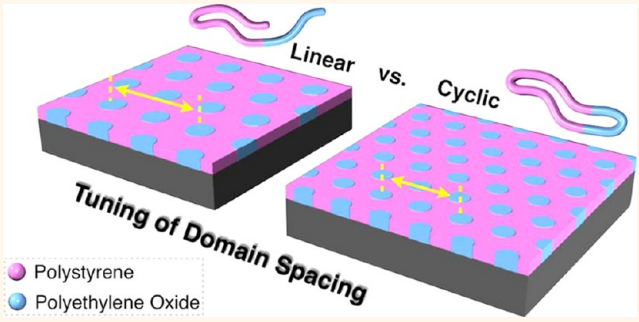

KEYWORDS: block copolymer · lithography · cyclic polymer · phase separation · self-assembly

The self-assembly of block copolymers (BCPs) for nanolithographic applications is driven by their unique characteristic to assemble on the length scale of individual polymer chains[1−11] to produce features of similar size to the most advanced top-down photolithographic techniques but at much reduced costs.[12] For future devices, the ability to pattern increasingly small features over large areas presents a difficult and expensive challenge, which has spurred major advances in block copolymer lithography.[13,14] Critical advances have been made in improving long-range order, in the selective removal of domains, and in understanding the assembly process.[15−21] Furthermore, extensive research in the area of directed self-assembly of BCPs has allowed for the patterning of the complex and arbitrary features required for fabrication of microelectronic devices with minimal top-down templating.[22−26] While these achievements represent significant steps toward adopting BCP lithography as a next-generation lithographic technique, the key to widespread commercial adoption is the ability to access sub-20 nm features[27,28] coupled with a high degree of versatility that can evolve to meet future industry demands.

A main advantage of BCP lithography as a robust next-generation lithographic technique is the ability to rationally design materials in order to control specific properties such as orientation, morphology, or feature size.[29−33] While the dimensions of individual domains and center-to-center spacing are theoretically determined by the overall molecular weight of the polymer, smaller domains are not obtained from lower molecular weight BCPs when the thermodynamic driving force for phase separation is insufficient to achieve well-defined domains. For these systems, disordered structures are obtained. One strategy to overcome this is the selection of monomers with increased χ values, such as polystyrene-*b*-poly(dimethyl siloxane); however these materials are synthetically challenging, and this approach is applicable only to a limited number of monomer pairs.[28,34] A general strategy for patterning regular arrays of

* Address correspondence to hawker@mrl.ucsb.edu.

Received for review September 12, 2012 and accepted November 24, 2012.

Published online November 29, 2012
10.1021/nn304217y

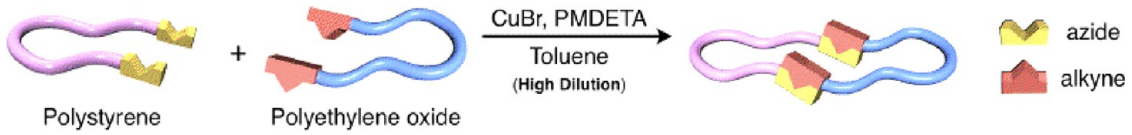

Figure 1. Graphical representation of the synthesis of cyclic block copolymers from telechelic functional homopolymer precursors by CuAAC.

features in the sub-20 nm regime from a wide selection of monomer pairs is therefore required.

A common characteristic of prior block copolymer lithography studies is the use of linear chains even though macromolecular architecture may also serve as a useful parameter for controlling molecular size and phase separation. In particular, cyclic macromolecules represent an interesting class of materials due to the lack of chain ends,[35−41] and when compared to linear polymers of similar molecular weights and composition, cyclic polymers display increased glass transition temperatures,[42] lower viscosities,[43,44] and, most significantly, decreased hydrodynamic volumes.[45] While all of these properties are potentially advantageous in block copolymer lithography, limited synthetic access has largely restricted exploration of cyclic polymers and, especially, cyclic block copolymers. To address these challenges, we have developed a general synthetic strategy for the preparation of cyclic block copolymers using a bimolecular homodifunctional approach. Traditionally, cyclization strategies employed small-molecule linkers;[58,67,68] however, by using a polymer instead of a small-molecule linker, intermolecular cyclization of two telechelic polymers of different chemical identity can be accomplished to yield cyclic diblock copolymers, as shown in Figure 1. This modular strategy permits cyclic block copolymers to be obtained with low polydispersities while also allowing different molecular weights and polymer backbones to be easily dictated by the starting linear polymers.

In this work, cylinder-forming cyclic PS-*b*-PEO was prepared by the bimolecular macrocyclization of N_3-PS-N_3 and alkyne-PEO-alkyne, and the thermal and self-assembly properties compared to a series of linear PS-*b*-PEO analogues. The cyclic and linear diblock copolymers were then deposited as thin films, and solvent was annealed to achieve phase separation with the domain sizes of the phase-separated thin films being characterized by atomic force microscopy and grazing incidence small-angle X-ray scattering.

RESULTS AND DISCUSSION

Synthesis of Cyclic Block Copolymers. While the synthesis of cyclic polymers has received increased attention in recent years,[46] the study of cyclic block copolymers is significantly less developed. This is unfortunate, as a number of reports have suggested that cyclic block copolymers can play a unique role in a variety of different applications. Recent studies have shown a dramatic increase in the thermal stability of flowerlike micelles formed from cyclic block copolymers,[47] a phenomenon also observed in the lipid bilayers of thermophilic *Archaea*, as well as higher critical micelle concentration values, smaller hydrodynamic radii, and lower average aggregation numbers.[48] Dating back to the 1960s, theoretical treatment of dilute solutions of ring polymers predicted that the hydrodynamic volumes of ring polymers are 1.12 times smaller than their linear counterparts at the theta condition.[49−52] Similarly, when cyclic diblock copolymers are compared to their linear analogues, the difference in domain spacing is expected to be much more significant, with theoretical predictions[53] and later computer simulations[54] suggesting a 33% decrease in the spacing of lamellae domains. These studies strongly suggest that the phase behavior and reduced domain size of cyclic diblock copolymers may offer a number of advantages in thin film studies and block copolymer lithography applications.

To facilitate these studies, a viable synthetic strategy for the preparation of cyclic block copolymers was required. Previously, synthetic routes to cyclic polymers can be broadly classified into two categories: either "ring expansion polymerizations" or "macrocyclization from linear precursors".[55,56] While ring expansion polymerizations have been very useful in the generation of large ring polymers and exotic gradient block copolymer structures, these methods are limited to select monomers and complex procedures.[44,57−60] As a more general route, macrocyclization from linear precursors is attractive, as it can be easily applied to a wide range of polymers with several synthetic strategies available.[61−63] Grayson and co-workers first demonstrated the macrocyclization of α-acetylene- and ω-azide-functionalized polymers,[65] including polystyrene-*b*-poly(methyl acrylate),[66] using a combination of controlled polymerization techniques and CuAAC. However, for the synthesis of cyclic block copolymers, unimolecular cyclization of heterodifunctional linear block polymers is so far restricted to monomers that are polymerized using the same controlled polymerization technique. Furthermore, careful purification of starting materials, protecting group strategies, and the synthesis of noncommercially available initiators limit the scope of this strategy.[67]

In keeping with the concept of a versatile synthetic platform and the ability to prepare cyclic block copolymers from repeat units with increased χ values, our

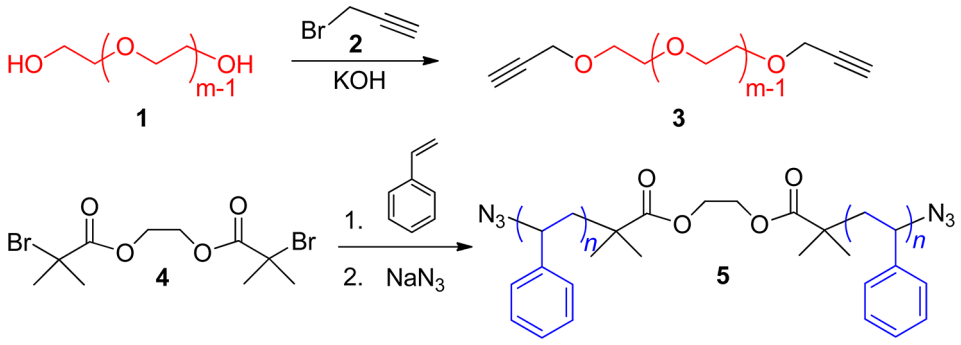

Scheme 1. Synthesis of alkyne-PEO-alkyne, 3, and N_3-PS-N_3, 5, linear precursors.

initial target was the preparation of cyclic PS-*b*-PEO diblock copolymers. Examining an intermolecular CuAAC coupling strategy between chain end functionalized linear homopolymers required the synthesis of difunctional PS and PEO derivatives with the molecular weights of the individual blocks chosen to be 5000 and 13 000 g/mol for PEO and PS, respectively. These molecular weights translate to a volume fraction of PEO equal to about 25%, which has been reported to give a cylindrical morphology of PEO cylinders embedded in a PS matrix.[32] For lithographic applications, the cylindrical morphology is desirable since the orientation can be controlled by solvent annealing conditions to be parallel or perpendicular to the substrate, allowing for the patterning of pillars, dots, or lines with the same material.

Because of the commercial availability of dihydroxy-terminated PEO and to reduce the number of synthetic steps, we chose to synthesize bisalkyne PEO and bisazide PS building blocks according to Scheme 1. Starting from a commercially available dihydroxy PEO (M_n = 5000 g/mol), nucleophilic substitution with propargyl bromide using potassium hydroxide as a base yielded polymer **3** after precipitation into hexanes. Complete conversion of the hydroxyl end groups to the alkyne was monitored and confirmed by ^{1}H NMR. The resulting homodifunctional PEO serves as the minor block and as a macromolecular linker for cyclization with the complementary bisazide PS described below.

The bisazide PS was synthesized from the difunctional initiator **4** *via* atom transfer radical polymerization (ATRP). The resulting bromo chain ends are observable by ^{1}H NMR and can be easily converted to the corresponding azido derivative by nucleophilic displacement with sodium azide. The polymerization was therefore conducted in neat styrene at 75 °C using *N,N,N′,N′,N″*-pentamethyldiethylenetriamine (PMDETA) and CuBr as the ligand and metal catalyst, respectively. Monomer conversion was monitored by ^{1}H NMR, and the reaction was terminated by quenching in liquid nitrogen and opening the flask to air after reaching the desired molecular weight of 13 000 g/mol with subsequent displacement by azide to give the desired bis(azido) polymer **5**, being confirmed by ^{1}H NMR (Figure 2a).

Synthesis and Characterization of cPS-*b*-PEO. The modular nature of this synthetic strategy therefore allows cyclic PS-*b*-PEO derivatives to be synthesized by the CuAAC intermolecular cyclization of **5** and **3**. In order to limit higher molecular weight polycondensation products, the cyclization reaction was conducted in dilute solution (125 mg of total polymer in 1 L of toluene) with a large catalytic loading of CuBr. ^{1}H NMR and FT-IR (Figure S11) confirmed complete consumption of the chain ends after two days at 60 °C, as can be seen in Figure 2. To further increase the efficiency of this strategy, a semibatch process was developed based on the stability of the triazole linking group under the cyclization conditions. Since complete reaction between the azide and alkyne end groups is observed with 48 h, a concentrated solution containing the linear precursors was added to the reaction vessel every 48 h over the course of a week. This allowed for a 5-fold increase in concentration with gram quantities of crude cyclic block copolymer being obtained in 1−2 L of solvent. Termination of the reaction was accomplished by opening the vessel to air, and the excess copper was removed by stirring with a 5 wt % solution of ethylenediaminetetraacetic acid (EDTA) in water.

The ^{1}H NMR spectra of the crude product (Figure 2c) reveals the complete disappearance of the diagnostic resonances for the N_3-PS-N_3 and alkyne-PEO-alkyne linear precursors, shown in Figure 3a and b, respectively. In the case of the cyclic block copolymer, **6**, the proton resonances from the methine protons in N_3-PS-N_3, **5** (*a*, Figure 2a) are shifted from 4.0 ppm to 5.3 ppm (*e*, Figure 2c) upon formation of the triazole ring, while the resonance for the methylene protons adjacent to the alkyne group in **3** (*c*, Figure 2b) is shifted from 4.2 ppm to 4.6 ppm (*f*, Figure 2c). The emergence of a unique resonance corresponding to the triazole proton was not observed by ^{1}H NMR and is likely obscured by the aromatic resonances originating from the PS block. The ratio of the integral values for *e*:*f* was found to be 1.09:2 in Figure 3c, which is close to the expected 1:2 ratio for the block copolymer. Combined with the lack

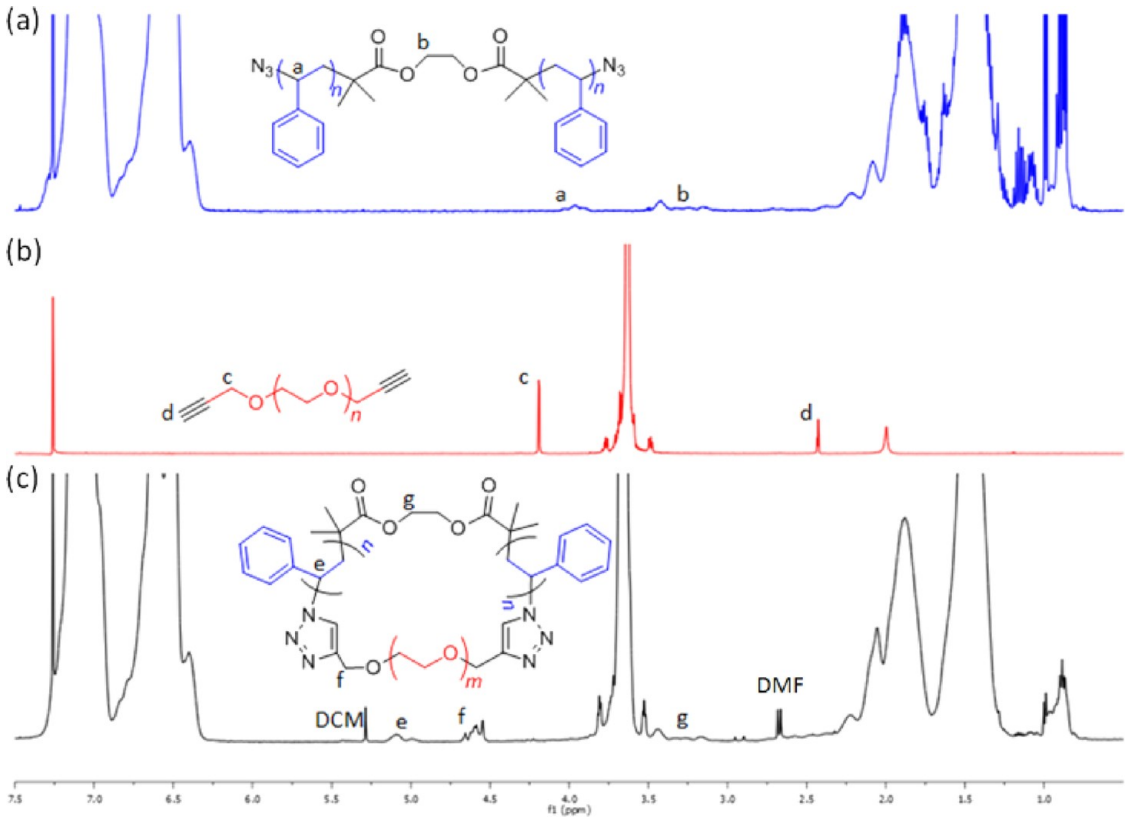

Figure 2. ^{1}H NMR of (a) N_3-PS-N_3, 5; (b) alkyne-PEO-alkyne, 3; and (c) cPS-*b*-PEO, 6.

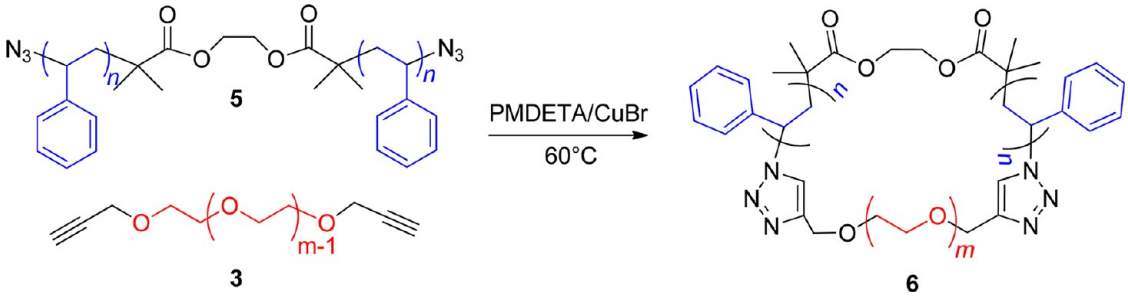

Scheme 2. Cyclization of alkyne-PEO-alkyne and N_3-PS-N_3 linear precursors to form cyclic PS-*b*-PEO, 6.

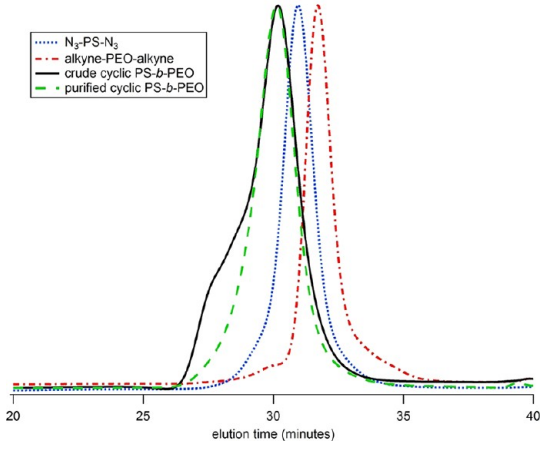

Figure 3. Gel permeation chromatograms of N_3-PS-N_3, alkyne-PEO-alkyne, and crude and purified cPS-*b*-PEO, 6.

of observable end groups, the integration values strongly suggest formation of a cyclic block copolymer. Similar evidence for macrocyclization was obtained from analysis of the crude product by infrared spectroscopy, which showed complete disappearance of the azide groups coupled with MALDI-mass spectrometry. For the latter, the complexity of the spectra due to the molecular weight dispersity in both the PS and PEO blocks precluded any quantification but was in agreement with the formation of triazole groups.

Comparison of gel permeation chromatographs for the reaction mixture and the two starting homopolymers revealed consumption of the linear precursors with emergence of a single peak at lower retention volumes, as shown by the solid line in Figure 3. The presence of a high molecular shoulder may be due

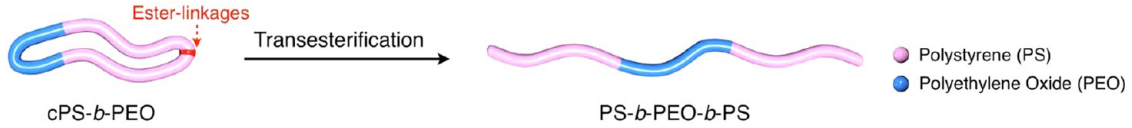

Scheme 3. Transesterification of cyclic PS-*b*-PEO to yield the conformational isomer PEO-*b*-PS-*b*-PEO.

to the formation of multiblock linear/cyclic polymers resulting from reaction of multiple linear precursors (*i.e.*, ABA or ABAB systems) or from incomplete cyclization of linear diblock copolymers. Monteiro *et al.* demonstrated that linear impurities with unreacted functionalities at the chain ends can be removed from the crude reaction mixture by coupling with a solid support containing azides or alkynes.[70] Our attempts to purify the crude material by this method were largely unsuccessful, with little reduction in the higher molecular weight shoulder, bolstering the idea that the higher molecular weight contaminants did not contain any unreacted azide or alkyne units and were therefore either linear polymers with no chain ends (incomplete functionalization of chain ends in starting material or loss during cycle formation) or higher order cyclic block copolymers. These higher molecular weight byproducts could however by easily removed *via* preparative gel permeation chromatography (GPC) to give the desired cyclic diblock copolymer. The resulting material possesses the molecular weight expected for a diblock copolymer formed from the linear precursors as well as a narrow PDI. ^{1}H NMR of the purified diblock copolymer yielded a spectrum nearly identical to the crude material but with integration values for the constituent blocks in full agreement with the desired structure.

As further confirmation of the cyclic structure, the specific incorporation of ester linkages in the PS block greatly facilitates direct comparison with a linear analogue, in this case an ABA triblock copolymer. Transesterification with methanol of the cPS-*b*-PEO diblock copolymer then gives the corresponding PS-*b*-PEO-*b*-PS triblock copolymer, as shown in Scheme 3. Comparison of the retention time of the purified material with the resulting triblock by GPC showed a clear shift to shorter retention volume, a result consistent with a change in molecular topology from a more compact cyclic structure to the expanded linear structure.

Synthesis of Linear PS-*b*-PEO. While the above hydrolysis study provides further proof for the formation of a cyclic diblock structure, in order to elucidate the effect of molecular topology on the domain size of nanophase-separated block copolymer thin films, it is more important to compare the cyclic PS-*b*-PEO to model systems based on the corresponding linear AB diblock copolymers. Two linear PS-*b*-PEO polymers were therefore synthesized as controls for the cyclic diblock copolymer. The rationale for the molecular weights chosen for the linear analogues is illustrated in Figure 4. The initial linear diblock copolymer, PS_{13K}-*b*-PEO_{5k}, has constituent blocks

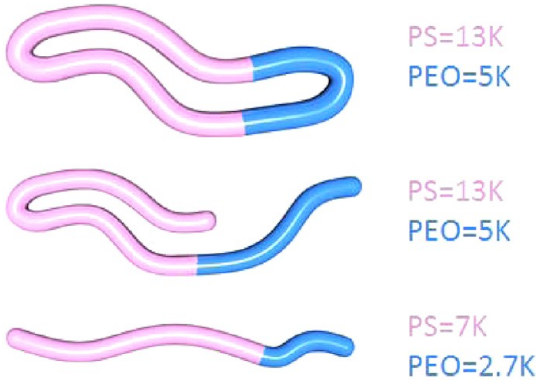

Figure 4. Visual representation of cPS-*b*-PEO and the corresponding full and half-molecular weight linear analogues.

with comparable molecular weights to the cyclic diblock copolymer and serves as a direct linear analogue. A second "half-molecular weight" linear BCP, PS_{7K}-*b*-$PEO_{2.7K}$, was synthesized to have blocks with molecular weights roughly half that of the cyclic BCP, emulating a case where the cyclic polymer is directly folded in the middle of each block.

The linear BCPs for these control studies were prepared by CuAAC of homopolymer precursors in a strategy similar to the synthesis of the cyclic BCP (Scheme 4). The monofunctional PS blocks were synthesized by ATRP using ethyl 2-bromo-2-methylpropionate as initiator with the bromo chain ends being converted to azides by nucleophilic displacement as described above. Similarly, the monofunctional PEO homopolymers were obtained by reaction of a monoalkyl PEO-OH with propargyl bromide. While monomethyl-PEO_{5K}-OH is available commercially, the $PEO_{2.7K}$-OH derivative was synthesized *via* living anionic polymerization of ethylene oxide using 2-propanol as the initiator. Linear PS-*b*-PEO diblock copolymers were then obtained by heating the appropriate PS-N_3 and PEO-alkyne homopolymers at 160 °C for 20 min in the presence of copper nanoparticles according to a procedure developed previously.[55] A slight excess of PS-N_3 was used to compensate for any unfunctionalized PS (see Supporting Information for characterization details).

Comparison of Thermal Properties of cPS-*b*-PEO with Linear Analogues. The semicrystalline nature of PEO prompted an investigation into the effect of architecture on the thermal properties of the cyclic and linear BCPs. Using differential scanning calorimetry, three heat–cool–heat cycles were therefore performed for each material with a heating and cooling rate of 2 °C/min. Representative heating cycles for the linear PS_{13K}-*b*-PEO_{5k} and

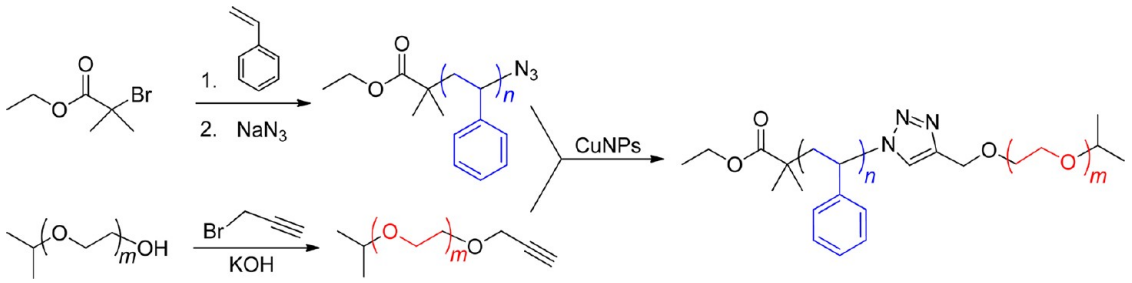

Scheme 4. Synthesis of linear PS-*b*-PEO diblock copolymer controls for comparison with cPS-*b*-PEO.

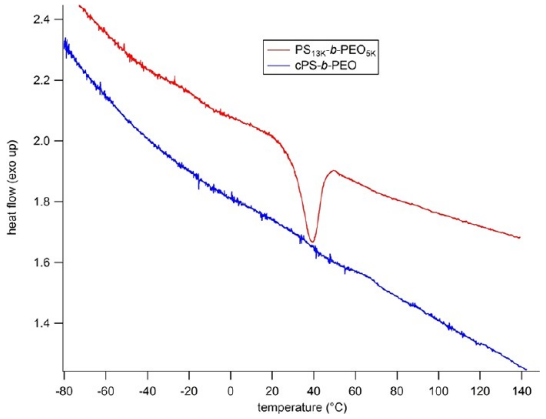

Figure 5. Differential scanning calorimetry traces for the linear PS_{13K}-*b*-PEO_{5K} (red line) and cyclic PS_{13K}-*b*-PEO_{5K} (blue line) diblock copolymers.

cyclic cPS_{13K}-*b*-PEO_{5k} materials are shown in Figure 5, with the PS_{13K}-*b*-PEO_{5k} linear analogue exhibiting an endotherm due to the melting of the semicrystalline PEO domains. In direct contrast, this transition is not observed in the cyclic material, which given the nearly identical molecular weights for the PEO blocks suggests a significant change in molecular architecture. Decreased chain mobility and induced curvature resulting from the topologically constrained cyclic architecture retard crystallization of the PEO block and provide further evidence for the unique behavior of the cyclic diblock system. It should also be noted that a melting transition was not observed for the lower molecular weight PS_{7K}-*b*-$PEO_{2.7K}$ derivatives, which is expected given the short length of the PEO block and lack of phase separation observed in the thin film studies.

Thin Film Studies. Thin films of the cyclic cPS-*b*-PEO diblock copolymer and the corresponding linear analogues were prepared by spin coating 2 wt % polymer solutions in toluene onto silicon substrates. The concentration of the polymer solutions and spin speed were kept constant for direct comparison of the cyclic and linear block copolymer thin films with all films having essentially the same thickness, and all were annealed in a toluene and a high humidity (~90% relative humidity) atmosphere for 48 h to allow for phase separation to occur. The resulting nanophase-separated thin films were characterized by atomic force microscopy (AFM) and grazing incidence X-ray scattering (GISAXS) in order to determine the effect of macromolecular architecture on nanophase-separated polymer thin films. AFM height images of the cyclic BCP and the full molecular weight linear BCP analogue are shown in Figure 6, with the cyclic PS-*b*-PEO (Figure 6a) displaying a considerable decrease in the diameter of the PEO cylinders embedded within the PS matrix compared to the PS_{13K}-*b*-PEO_{5K} linear analogue (Figure 6b). This result is consistent with the more compact structure and additional constraints resulting from the lack of chain ends in the cyclic system. Qualitative analysis of the periodicities for the ordered structures were extracted from the 2-D Fourier transform (FT) of the AFM images (shown as insets) and found to be *ca.* 20 nm and *ca.* 25 nm for cPS-*b*-PEO and PS_{13K}-*b*-PEO_{5K}, respectively. To further quantify the domain spacing and remove any artifacts from surface effects or AFM tip-induced error, grazing incidence X-ray scattering experiments were conducted to accurately measure the effect of cyclization on domain spacing through the entire thickness of the film. For the cyclic diblock copolymer, a first-order reflection at $q_y = 0.03216$ Å^{-1} and a second peak at $q_y = 0.05488$ Å^{-1} were observed, which correspond to a *d*-spacing of 19.5 nm. In direct contrast, the linear PS_{13K}-*b*-PEO_{5K} analogue showed a first-order peak $q_y = 0.0242$ Å^{-1}, corresponding to a *d*-spacing of 25.9 nm, and clearly demonstrates that the features for the cyclic block copolymer thin film are about 33% smaller than the full molecular weight linear analogue. Notably, microphase separation was not observed for the half molecular weight linear analogue PS_{7K}-*b*-PEO_{3K}. This is likely due to an insufficient driving force for phase separation *via* solvent annealing and highlights the importance of cyclic architectures for targeting smaller feature sizes while at the same time maintaining increased χN values for phase separation.

CONCLUSIONS

We have successfully demonstrated a general and modular approach to the synthesis of gram quantities of cyclic block copolymers by Cu-catalyzed azide/alkyne coupling of α,ω-azide-functionalized PS and α,ω-alkyne PEO homopolymers. Compared to their linear analogues, the cyclic BCPs yield phase-separated

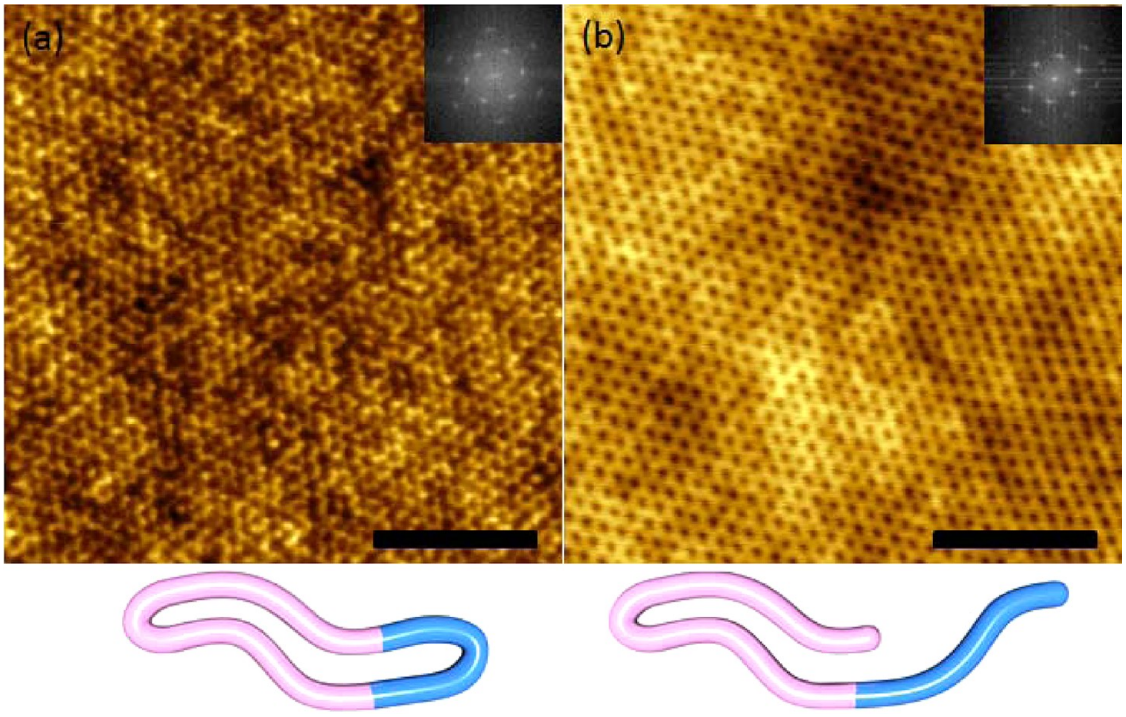

Figure 6. Atomic force microscopy height images for (a) cyclic PS_{13K}-*b*-PEO_{5K} and (b) PS_{13K}-*b*-PEO_{5K} diblock copolymers. Scale bars are 250 nm.

thin films with feature sizes less than 20 nm, which corresponds to a decrease of ~33%. These results demonstrate that macromolecular architecture should be consider as an important design feature for controlling feature size in block copolymer lithography, especially in the important sub-20 nm size regime.

METHODS

Materials were characterized by ^{1}H nuclear magnetic resonance (NMR) spectroscopy, using a Bruker 500 MHz spectrometer with the residual solvent peak as an internal reference. Gel permeation chromatography was performed in chloroform with 0.25 vol % TEA as an additive on a Waters chromatograph equipped with four 5 μm Waters columns (300 × 7.7 mm) connected in series with increasing pore size (100, 1000, 10 000, 1 000 000 Å) coupled to a Waters 2414 differential refractometer. The molecular weights of the polymers were calculated relative to linear PS or PEO standards. Modulated differential scanning calorimetry (MDSC) experiments were performed on a TA Instruments Q2000 MDSC with a ramp rate of 2 °C/min. Infrared spectra (IR) were acquired on a Perkin-Elmer Spectrum 100 with a Universal ATR sampling accessory.

Atomic Force Microscopy. Tapping mode AFM experiments were performed using a MFP-3D system (Asylum Research, Santa Barabara, CA, USA). The measurements were conducted using commercial Si cantilevers with a nominal spring constant and resonance frequency of 3.0 N/m and 62 kHz, respectively (FORTA, Applied Nanostructures, Santa Clara, CA, USA). The height and phase images were acquired simultaneously at the set point ratio A/A_0 = 0.90−0.95, where A and A_0 are the "tapping" and "free" cantilever amplitudes, respectively.

Grazing Incidence Small-Angle X-ray Scattering. GISAXS experiments for the cyclic BCP thin films were carried out at the 4C2 beamlines at the Pohang Accelerator Laboratory (PAL), Korea. Two-dimensional GISAXS patterns were recorded using a CCD detector positioned at the end of a vacuum guide tube when the X-rays pass through the BCP thin films under vacuum, where the operating conditions were set to a wavelength of 1.38 Å and a sample-to-detector distance of 2.2 m. Characterization of the linear analogue thin films was conducted at UCSB in the beamline of a home-built spectrometer consisting of a fine-focus XENOCS Genix 50W X-ray microsource and Bruker HI-STAR multiwire area detector.

Telechelic Dibromo-Terminated Polystyrene. Glassware and stir bar were dried at 145−155 °C for 24 h, fitted with rubber septa, and cooled under a flow of dry nitrogen. To a 100 mL Schlenk flask were added styrene (0.13 mol, 13.6 g), ethylene bis-(2-bromoisobutyrate) (0.75 mmol, 0.268 g), and PMDETA (2.8 mmol, 0.491 g). The reaction mixture was degassed by three freeze−pump−thaw cycles. On the third freeze, CuBr (2.2 mmol, 0.313 g) and $CuBr_2$ (0.9 mmol, 0.200 g) were added under a flow of dry nitrogen. The reaction mixture was stirred at room temperature for 15 min to allow formation of the copper catalyst, and then the polymerization was heated at 75 °C for 10 h and terminated by quenching into liquid nitrogen after a monomer conversion of 58% was reached. The resulting polymer was obtained after two precipitations into hexanes and characterized by GPC (M_n = 13 000 g/mol; PDI = 1.06) and ^{1}H NMR: δ (ppm) 1.05−2.57 (m, $-CH_2CH(Ph)-$), 4.35−4.62 (m, $-CH(Ph)-Br$), 3.05−3.47 (m, $-(C{=}O)CH_2CH_2(C{=}O)-$), 6.25−7.41 (m, $-CH_2CH(C_6H_5)-$).

Telechelic Bisazido-Terminated Polystyrene (5). To a 50 mL round-bottom flask were charged 20 mL of dimethylformamide, telechelic dibromo-terminated polystyrene (0.36 mmol, 5.0 g), and sodium azide (7.1 mmol, 0.46 g). The reaction was stirred at room temperature for 24 h, and the resulting azide-functionalized polystyrene was obtained by precipitation into methanol. ^{1}H NMR revealed the polymer to be >95% functionalized. ^{1}H NMR: δ (ppm) 1.05−2.60 (m, $-CH_2CH(Ph)-$), 3.83−4.07 (m, $-CH(Ph)-N_3$), 3.05−3.45 (m, $-(C{=}O)CH_2CH_2(C{=}O)-$), 6.20−7.49 (m, $-CH_2CH(C_6H_5)-$).

Propargyl-Telechelic Polyethylene Oxide (3). To a 100 mL round-bottom flask were added 50 mL of toluene, telechelic

hydroxyl-terminated poly(ethylene oxide), M_n = 5000 g/mol and PDI of 1.04 (1.0 mmol, 5.0 g), propargyl bromide (80 wt % in toluene) (21 mmol, 3.0 g), and crushed potassium hydroxide pellets (10 mmol, 0.58 g). The reaction mixture was stirred at 60 °C for 24 h, and the KOH pellets were removed by vacuum filtration. The bis-propargyl-functionalized polymer was obtained by precipitation into hexanes. Characterization by GPC showed a M_n = 5000 g/mol and PDI of 1.04 using PEO standards. ^{1}H NMR revealed the polymer to be >95% functionalized. ^{1}H NMR: δ (ppm) 2.40−2.49 (s, −C≡C*H*), 3.35−4.03 (s br, −OCH_2), 4.14−4.26 (s, −CH_2).

Cyclic Polystyrene-*block*-polyethylene Oxide (6). To a 2 L round-bottom flask was charged 1.5 L of toluene, telechelic bisazide PS (1.1×10^{-5} mol, 0.128 g), telechelic bisalkyne PEO (1.1×10^{-5} mol, 0.055 g), and PMDETA (7.5×10^{-3} mol, 1.3 g). The reaction mixture was sparged with dry nitrogen for 20 min while stirring. CuBr (5.0×10^{-3} mol, 0.722 g) was then added to the flask, and stirring continued for 20 min to allow the copper catalyst complex to form. The reaction mixture was then heated at 60 °C. After 48 h, 1 mL of a degassed solution in toluene containing 128 mg of bisazide PS and 55 mg of bisalkyne PEO was added *via* syringe. This process was repeated every 48 h for three repetitions. The reaction was terminated by opening to air and stirring with 100 mL of brine for 0.5 h followed by 100 mL of 5 wt % EDTA for 0.5 h. The organic layer was decanted and evaporated to dryness, while the aqueous layer was washed with 50 mL of dichloromethane twice. The organic fractions were combined and washed with 5 wt % EDTA and brine to remove any excess copper. The crude product was obtained as a slightly yellow waxy solid after precipitation into hexanes. The crude product was then purified by preparative GPC to remove higher molecular weight polymers to give the monocyclic product. Characterization by ^{1}H NMR revealed complete consumption of the azide and alkynes, and no starting materials remained, as evidenced by GPC (M_n = 13 900; PDI = 1.08). ^{1}H NMR: δ (ppm) 1.09−2.31 (m, −CH_2C*H*(Ph)−), 3.07−3.48 (m, −(C═O)CH_2CH_2(C═O)−), 3.56−3.76 (s br, −OCH_2), 4.51−4.68 (m, −CH_2), 4.92−5.16 (m, −C*H*(Ph)-triazole), 6.26−7.37 (m, −CH_2CH(C$_6$H$_5$)−).

Conflict of Interest: The authors declare no competing financial interest.

Supporting Information Available: Synthesis of linear block copolymers. ^{1}H NMR and GPC of linear block copolymers. FT-IR spectroscopy of linear precursors and the cyclic product. Characterization of thin films by GISAXS. This material is available free of charge *via* the Internet at http://pubs.acs.org.

Acknowledgment. This work was supported by the Microelectronics Advanced Semiconductor Research Corporation (SMARCO) and its Focus Center Research Program (FCRP)—Center for Functional Engineered NanoArchitectonics (FENA) (J.E.P.) as well as the UCSB Materials Research Laboratory (NSF DMR 1121053) (J.E.P., K.O., D.M., K.S., and C.J.H.). The authors would also like to thank Professor Joona Bang and Hyungjung Jung for preparing the 2-D GISAXS data.

REFERENCES AND NOTES

1. Park, M.; Harrison, C.; Chaikin, P. M.; Register, R. A.; Adamson, D. H. Block Copolymer Lithography: Periodic Arrays of $\sim 10^{11}$ Holes in 1 Square Centimeter. *Science* **1997**, *276*, 1401–1404.
2. Bang, J.; Jeong, U.; Ryu, D. Y.; Russell, T. P.; Hawker, C. J. Block Copolymer Nanolithography: Translation of Molecular Level Control to Nanoscale Patterns. *Adv. Mater.* **2009**, *21*, 4769–4792.
3. Whitesides, G. M.; Mathias, J. P.; Seto, C. T. Molecular Self-Assembly and Nanochemistry: A Chemical Strategy for the Synthesis of Nanostructures. *Science* **1991**, *254*, 1312–1319.
4. Kim, S. O.; Solak, H. H.; Stoykovich, M. P.; Ferrier, N. J.; de Pablo, J. J.; Nealey, P. F. Epitaxial Self-Assembly of Block Copolymers on Lithographically Defined Nanopatterned Substrates. *Nature* **2003**, *424*, 411–414.
5. Chai, J.; Wang, D.; Fan, X.; Buriak, J. M. Assembly of Aligned Linear Metallic Patterns on Silicon. *Nat. Nanotechnol.* **2007**, *2*, 500–506.
6. Albert, J. N. L.; Epps, T. H., III. Self-Assembly of Block Copolymer Thin Films. *Mater. Today* **2010**, *13*, 24–33.
7. Bosworth, J. K.; Black, C. T.; Ober, C. K. Selective Area Control of Self-Assembled Pattern Architecture Using a Lithographically Patternable Block Copolymer. *ACS Nano* **2009**, *3*, 1761–1766.
8. Ruiz, R.; Dobisz, E.; Albrecht, T. R. Rectangular Patterns Using Block Copolymer Directed Assembly for High Bit Aspect Ratio Patterned Media. *ACS Nano* **2011**, *5*, 79–84.
9. Hayward, R. C.; Chmelka, B. F.; Kramer, E. J. Crosslinked Poly(styrene)-*block*-Poly(2-vinylpyridine) Thin Films as Swellable Templates for Mesostructured Silica and Titania. *Adv. Mater.* **2005**, *17*, 2591–2595.
10. Shin, K.; Leach, K. A.; Goldbach, J. T.; Kim, D. H.; Jho, J. Y.; Tuominen, M.; Hawker, C. J.; Russell, T. P. A Simple Route to Metal Nanodots and Nanoporous Metal Films. *Nano Lett.* **2002**, *2*, 933–936.
11. Hu, Y.; Chen, D.; Park, S.; Emrick, T.; Russell, T. P. Guided Assemblies of Ferritin Nanocages: Highly Ordered Arrays of Monodisperse Nanoscopic Elements. *Adv. Mater.* **2010**, *22*, 2583–2587.
12. Stoykovich, M. P.; Kang, H.; Daoulas, K. C.; Liu, G.; Liu, C.-C; de Pablo, J. J.; D.Müller, M.; Nealey, P. F. Directed Self-Assembly of Block Copolymers for Nanolithography: Fabrication of Isolated Features and Essential Integrated Circuit Geometries. *ACS Nano* **2007**, *1*, 168–175.
13. Hawker, C. J.; Russell, T. P. Block Copolymer Lithography: Merging "Bottom-Up" with "Top-Down" Processes. *MRS Bull.* **2005**, *30*, 952–966.
14. Stoykovich, M. P.; Nealey, P. F. Block Copolymers and Conventional Lithography. *Mater. Today* **2006**, *9*, 20–29.
15. Park, S.; Lee, D. H.; Xu, J.; Kim, B.; Hong, S. W.; Jeong, U.; Xu, T.; Russell, T. P. Macroscopic 10-Terabit-per-Square-Inch Arrays from Block Copolymers with Lateral Order. *Science* **2009**, *323*, 1030–1033.
16. Kang, M.; Moon, B. Synthesis of Photocleavable Poly(styrene-*block*-ethylene oxide) and Its Self-Assembly into Nanoporous Thin Films. *Macromolecules* **2009**, *42*, 455–458.
17. Yurt, S.; Anyanwu, U. K.; Scheintaub, J. R.; Coughlin, E. B.; Venkataraman, D. Scission of Diblock Copolymeres into Their Constituent Blocks. *Macromolecules* **2006**, *39*, 1670–1672.
18. Zhang, M. F.; Yang, L.; Yurt, S.; Misner, M. J.; Chen, J. T.; Coughlin, E. B.; Venkataraman, D.; Russell, T. P. Highly Ordered Nanoporous Thin Films from Cleavable Polystyrene-*block*-Poly(ethylene oxide). *Adv. Mater.* **2007**, *19*, 1571.
19. Tang, C.; Sivanandan, K.; Stahl, B. C.; Fredrickson, G. H.; Kramer, E. J.; Hawker, C. J. Multiple Nanoscale Templates by Orthogonal Degradation of a Supramolecular Block Copolymer Lithographic System. *ACS Nano* **2010**, *4*, 285–291.
20. Ryu, J.-H.; Park, S.; Kim, B.; Klaikherd, A.; Russell, T. P.; Thayumanavan, S. Highly Ordered Gold Nanotubes Using Thiols at a Cleavable Block Copolymer Interface. *J. Am. Chem. Soc.* **2009**, *131*, 9870.
21. Glassner, M.; Blinco, J. P.; Barner-Kowollik, C. Formation of Nanoporous Materials *via* Mild Retro-Diels-Alder Chemistry. *Polym. Chem.* **2011**, *2*, 83–87.
22. Jung, Y. S.; Ross, C. A. Orientation Controlled Self-Assembled Nanolithography Using a Polystyrene-Polydimethylsiloxane Block Copolymer. *Nano Lett.* **2007**, *7*, 2046–2050.
23. Stoykovich, M. P.; Müller, M.; Kim, S. O.; Solak, H. H.; Edwards, E. W.; de Pablo, J. J.; Nealey, P. F. Directed Assembly of Block Copolymer Blends into Nonregular Device-Oriented Structures. *Science* **2005**, *308*, 1442–1446.
24. Cheng, J. Y.; Mayes, A. M.; Ross, C. A. Nanostructure Engineering by Templated Self-Assembly of Block Copolymers. *Nat. Mater.* **2004**, *3*, 823–828.

25. Yang, J. K. W.; Jung, Y. S.; Chang, J.-B.; Mickiewicz, R. A.; Alexander-Katz, A.; Ross, C. A.; Berggren, K. K. Complex Self-Assembled Patterns Using Sparse Commensurate Templates with Locally Varying Motifs. *Nat. Nanotechnol.* **2010**, *5*, 256–260.
26. Ruiz, R.; Kang, H.; Detcheverry, F. A.; Dobisz, E.; Kercher, D. S.; Albrecht, T. R.; de Pablo, J. J.; Nealey, P. F. Density Multiplication and Improved Lithography by Directed Block Copolymer Assembly. *Science* **2008**, *321*, 936–939.
27. Park, H. J.; Kang, M.-Gyu; Guo, L. J. Large Area High Density Sub-20 nm SiO_2 Nanostructures Fabricated by Block Copolymer Template for Nanoimprint Lithography. *ACS Nano* **2009**, *3*, 2601–2608.
28. Voet, V. S. D.; Pick, T. E.; Park, S.-M.; Moritz, M.; Hammack, A. T.; Urban, J. J.; Ogletree, D. F.; Olynick, D. L.; Helms, B. A. Interface Segregating Fluoralkyl-Modified Polymers for High-Fidelity Block Copolymer Nanoimprint Lithography. *J. Am. Chem. Soc.* **2011**, *133*, 2812–2815.
29. Tang, C.; Lennon, E. M.; Fredrickson, G. H.; Kramer, E. J.; Hawker, C. J. Evolution of Block Copolymer Lithography to Highly Ordered Square Arrays. *Science* **2008**, *322*, 429–432.
30. Bates, F. S.; Fredrickson, G. H. Block Copolymers — Designer Soft Materials. *Phys. Today* **1999**, *February*, 32–38.
31. Bang, J.; Kim, B. J.; Stein, G. E.; Russell, T. P.; Li, X.; Wang, J.; Kramer, E. J.; Hawker, C. J. Effect of Humidity on the Ordering of PEO-Based Copolymer Thin Films. *Macromolecules* **2007**, *40*, 7019–7025.
32. Kim, S. H.; Misner, M. J.; Xu, T.; Kimura, M.; Russell, T. P. Highly Oriented and Ordered Arrays from Block Copolymers *via* Solvent Evaporation. *Adv. Mater.* **2004**, *16*, 226–231.
33. Tang, C.; Bang, J.; Stein, G. E.; Fredrickson, G. H.; Hawker, C. J.; Kramer, E. J.; Sprung, M.; Wang, J. Square Packing and Structural Arrangement of ABC Triblock Copolymer Spheres in Thin Films. *Macromolecules* **2008**, *41*, 4328–4339.
34. Jung, Y. S.; Chang, J. B.; Verploegen, E.; Berggren, K. K.; Ross, C. A. A Path to Ultranarrow Patterns Using Self-Assembled Lithography. *Nano Lett.* **2010**, *10*, 1000–1005.
35. Semlyen, J. A. *Cyclic Polymers*, 2nd ed.; Springer: Berlin, 2001.
36. McLeish, T. Polymers without Beginning or End. *Science* **2002**, *297*, 2005–2006.
37. Yamamoto, T.; Tezuka, Y. Topological Polymer Chemistry: A Cyclic Approach toward Novel Polymer Properties and Functions. *Polym. Chem.* **2011**, *2*, 1930–1941.
38. McLeish, T. Polymer Dynamics: Floored by the Rings. *Nat. Mater.* **2008**, *7*, 933–935.
39. Hoskins, J. N.; Grayson, S. M. Cyclic Polyesters: Synthetic Approaches and Potential Applications. *Polym. Chem.* **2011**, *2*, 289–299.
40. Semlyen, J. A.; Wood, B. R.; Hodge, P. Cyclic Polymers: Past. *Present and Future. Polym. Adv. Tech.* **1994**, *5*, 473–478.
41. Kricheldorf, H. R. Cyclic Polymers: Synthetic Strategies and Physical Properties. *J. Polym. Sci., Part A: Polym. Chem.* **2010**, *48*, 251–284.
42. Xu, X.; Zhou, N.; Zhu, J.; Tu, Y.; Zhang, Z.; Cheng, Z.; Zhu, X. The First Examples of Main-Chain Cyclic Azobenzene Polymers. *Macromol. Rapid Commun.* **2010**, *31*, 1791–1797.
43. Kapnistos, M.; Lang, M.; Vlassopoulos, D.; Pyckhout-Hintzen, W.; Richter, D.; Cho, D.; Chang, T.; Rubinstein, M. Unexpected Power-Law Stress Relaxation of Entangled Ring Polymers. *Nat. Mater.* **2008**, *7*, 997–1002.
44. Culkin, D. A.; Jeong, W.; Csihony, S.; Gomez, E. D.; Balsara, N. P.; Hedrick, J. L.; Waymouth, R. M. Zwitterionic Polymerization of Lactide to Cyclic Poly(lactide) by Using N-Heterocyclic Carbene Organocatalysts. *Angew. Chem., Int. Ed.* **2007**, *46*, 2627–2630.
45. Lonsdale, D. E.; Monteiro, M. J. Various Polystyrene Topologies Built from Tailored Cyclic Polystyrene *via* CuAAC Reactions. *Chem. Commun.* **2010**, *46*, 7945–7947.
46. Jia, Z.; Monteiro, M. J. Cyclic Polymers: Methods and Strategies. *J. Polym. Sci., Part A: Polym. Chem.* **2012**, *50*, 2058–2097.
47. Honda, S.; Yamamoto, T.; Tezuka, Y. Topology-Directed Control on Thermal Stability: Micelles Formed from Linear and Cyclized Amphiphilic Block Copolymers. *J. Am. Chem. Soc.* **2010**, *132*, 10251–10253.
48. Ge, Z.; Zhou, Y.; Xu, J.; Liu, H.; Chen, D.; Liu, S. High Efficiency Preparation of Macrocyclic Diblock Copolymers *via* Selective Click Reaction in Micellar Media. *J. Am. Chem. Soc.* **2009**, *131*, 1628–1629.
49. Fukatsu, M.; Kurata, M. Hydrodynamic Properties of Flexible-Ring Macromolecules. *J. Chem. Phys.* **1966**, *44*, 4539–4545.
50. Hadziioannou, G.; Cotts, P. M; ten Brinke, G.; Han, C. C.; Lutz, P.; Strazielle, C.; Rempp, P.; Kovacs, A. J. Thermodynamic and Hydrodynamic Properties of Dilute-Solutions of Cyclic and Linear Polystyrenes. *Macromolecules* **1987**, *20*, 493–497.
51. Roovers, J. Dilute-Solution Properties of Ring Polystyrenes. *J. Polym. Sci., Polym. Phys. Ed.* **1985**, *23*, 1117–1126.
52. Lescanec, R. L.; Hajduk, D. A.; Kim, G. Y.; Gan, Y.; Yin, R.; Gruner, S. M.; Hogen-Esch, T. E.; Thomas, E. L. Comparison of the Lamellar Morphology of Microphase-Separated Cyclic Block Copolymers and Their Linear Precursors. *Macromolecules* **1995**, *28*, 3485–3489.
53. Marko, J. F. Microphase Separation of Block Copolymer Rings. *Macromolecules* **1993**, *26*, 1442–1444.
54. Qian, H.; Lu, Z. Y.; Chen, L. J.; Li, Z. S.; Sun, C. C. Computer Simulation of Cyclic Block Copolymer Microphase Separation. *Macromolecules* **2005**, *38*, 1395–1401.
55. Pressly, E. D.; Amir, R. J.; Hawker, C. J. Rapid Synthesis of Block and Cyclic Copolymers *via* Click Chemistry in the Presence of Copper Nanoparticles. *J. Polym. Sci., Part A: Polym. Chem.* **2011**, *49*, 814–819.
56. Laurent, B. A.; Grayson, S. M. Synthetic Approaches for the Preparation of Cyclic Polymers. *Chem. Soc. Rev.* **2009**, *38*, 2202–2213.
57. Bielawski, C. W.; Benitez, D.; Grubbs, R. H. An "Endless" Route to Cyclic Polymers. *Science* **2002**, *297*, 2041–2044.
58. Boydston, A. J.; Xia, Y.; Kornfield, J. A.; Gorodetskaya, I. A; Grubbs, R. H. Cyclic Ruthenium-Alkylidene Catalysts for Ring-Expansion Metathesis Polymerization. *J. Am. Chem. Soc.* **2008**, *130*, 12775–12782.
59. Shin, E. J.; Brown, H. A; Gonzalez, S.; Jeong, W.; Hedrick, J. L.; Waymouth, R. M. Zwitterionic Copolymerization: Synthesis of Cyclic Gradient Copolymers. *Angew. Chem., Int. Ed.* **2011**, *50*, 6388–6391.
60. Lee, C.-U.; Smart, T. P.; Guo, L.; Epps, T. H., III; Zhang, D. Synthesis and Characterization of Amphiphilic Cyclic Diblock Copolypeptoids from *N*-Heterocyclic Carbene-Mediated Zwitterionic Polymerization of *N*-Substituted *N*-Carboxyanhydride. *Macromolecules* **2011**, *44*, 9574–9585.
61. Stanford, M. J.; Pflughaupt, R. L.; Dove, A. P. Synthesis of Stereoregular Cyclic Poly(lactide)s *via* "Thiol-Ene" Click Chemistry. *Macromolecules* **2010**, *43*, 6538–6541.
62. Quirk, R. P.; Wang, S-F; Foster, M. D. Synthesis of Cyclic Polystyrenes Using Living Anionic Polymerization and Metathesis Ring-Closure. *Macromolecules* **2011**, *44*, 7538–7545.
63. Nicolay, R.; Matyjaszewski, K. Synthesis of Cyclic (Co)polymers by Atom Transfer Radical Cross-Coupling and Ring Expansion by Nitroxide-Mediated Polymerization. *Macromolecules* **2011**, *44*, 240–247.
64. Laurent, B. A.; Grayson, S. M. Synthesis of Cyclic Amphiphilic Homopolymers and Their Potential Applications as Polymeric Micelles. *Polym. Chem.* **2012**, *3*, 1846–1855.
65. Laurent, B. A.; Grayson, S. M. An Efficient Route to Well-Defined Macrocyclic Polymers *via* "Click" Cyclization. *J. Am. Chem. Soc.* **2006**, *128*, 4238–4239.
66. Eugene, D. M.; Grayson, S. M. Efficient Preparation of Cyclic Poly(methyl acrylate)-*block*-Poly(styrene) by Combination of Atom Transfer Radical Polymerization and Click Cyclization. *Macromolecules* **2008**, *41*, 5082–5084.
67. Touris, A.; Hadjichristidis, N. Cyclic and Multiblock Polystrene-*block*-Polyisoprene Copolymers by Combining

Anionic Polymerization and Azide/Alkyne "Click" Chemistry. *Macromolecules* **2011**, *44*, 1969–1976.
68. Clark, P. G.; Guidry, E. N.; Chan, W. Y.; Steinmetz, W. E.; Grubbs, R. H. Synthesis of a Molecular Charm Bracelet *via* Click Cyclization and Olefin Metathesis Clipping. *J. Am. Chem. Soc.* **2010**, *132*, 3405–3412.
69. Schulz, M.; Tanner, S.; Barqawi, H.; Binder, W. H. Macrocyclization of Polymers *via* Ring-Closing Metathesis and Azide/Alkyne "Click" Reactions: An Approach to Cyclic Polyisobutylenes. *J. Polym. Sci., Part A: Polym. Chem.* **2010**, *48*, 671–680.
70. Urbani, C. N.; Bell, C. A.; Lonsdale, D.; Whittaker, M. R.; Monteiro, M. J. Reactive Alkyne and Azide Solid Supports to Increase Purity of Novel Polymeric Stars and Dendrimers *via* the "Click" Reaction. *Macromolecules* **2007**, *40*, 7056–7059.